COMPDYN 2011
III ECCOMAS Thematic Conference on
Computational Methods in Structural Dynamics and Earthquake Engineering
M. Papadrakakis, M. Fragiadakis, V. Plevris (eds.)
Corfu, Greece, 26–28 May 2011

MAXWELL NONLINEAR SLIDER MODEL FOR SEISMIC RESPONSE PREDICTION OF SEMI-ACTIVE CONTROLLED MAGNETO-RHEOLOGICAL DAMPERS

Yunbyeong Chae[1], James M. Ricles[1], and Richard Sause[1]

[1] Lehigh University, 117 ATLSS Drive, Bethlehem, PA 18015 USA
e-mail: yuc206@lehigh.edu, jmr5@lehigh.edu, rs0c@lehigh.edu

Keywords: Magneto-Rheological (MR) damper, Structural Dynamics, Real-Time Hybrid Simulation, Dynamics of Electromagnetism

Abstract. *Magneto-rheological (MR) dampers are a promising device for seismic hazard mitigation of structural systems due to their ability to adaptively vary their damping characteristics using an appropriate control law. A majority of past research has involved small-scale MR dampers. In order to investigate the dynamic behavior of large-scale MR dampers, characterization tests have been conducted on large-scale MR dampers at the Lehigh NEES equipment site. A new MR damper model, called the Maxwell Nonlinear Slider Model (MNS), was developed using the data from these tests. The new MR damper model can independently describe the pre-yield and post-yield behavior of an MR damper, making it easier to identify the model parameters. The new damper model utilizes the Hershel-Bulkley visco-plasticity formulation to describe the post-yield behavior of the damper, and possesses the characteristics of a non-Newtonian fluid, i.e., shear thinning and thickening behavior of MR fluid. The effects of the dynamics of an MR damper associated with variable current input from a semi-active control law is integrated into the model by a nonlinear differential equation describing the eddy current effect and the magnetization behavior of damper materials. The accuracy of the new MR damper model is compared with other existing models, such as the Bouc-Wen and hyperbolic tangent models. Experimental studies are performed involving real-time hybrid simulations of complete structural systems, where MR dampers in the structure are subjected to realistic demands associated with the design basis and maximum considered earthquakes. Comparisons of the measured hysteretic response of the large-scale dampers in the tests with the predicted behavior by the MNS damper model show that the new model is able to achieve a high degree of accuracy compared to existing MR damper models under earthquake loading conditions. The MNS model enables accurate nonlinear time history analysis for the response prediction of structural systems with MR dampers to be performed.*

1 INTRODUCTION

Magneto-rheological (MR) dampers are devices which can have their characteristics vary by changing the input current to the damper. The MR damper force depends on the yield stress of the MR fluid inside the damper, which is a function of the input current to the damper. When an MR fluid is subjected to a magnetic field, the iron particles in the fluid are aligned and form linear chains parallel to the field, changing the state of the fluid to a semi-solid, which in turn increases the fluid viscosity and restricts the fluid movement through the orifices in an MR damper. This results in changing the yield stress of the MR fluid. MR dampers can be used for seismic hazard mitigation by incorporating these devices into structures. Dyke et al. [1] studied the feasibility of an MR damper as a means of suppressing vibrations in a structure using a clipped optimal controller algorithm. Thereafter, numerous researchers have studied the behavior of structures with passively or semi-actively controlled MR dampers [2-4]. Most of those studies involved small-scale MR dampers.

Large-scale MR dampers have been experimentally investigated by numerous researchers [5-8]. Numerous damper models have been developed to predict the behavior of MR dampers [9-11]. Among these models, the Bouc-Wen model [9] and hyperbolic tangent model [11] are popular, and have been used by Yang et al. [12] and Bass and Christenson [8] to model large-scale MR dampers. Both the Bouc-Wen model and the hyperbolic tangent model can accurately predict the frequency dependent behavior and roll-off phenomenon that occurs at low velocities in MR dampers. However, due to the complexity of these nonlinear models the estimation of the model parameters can be difficult. Moreover, it is difficult for these models to accurately describe the shear thinning or thickening behavior that occurs in the MR fluid [6] during the post yield response when high velocities can develop in the damper. In both the Bouc-Wen and hyperbolic tangent models the post-yield behavior is predominantly described by a linear dashpot; hence, the post-yield behavior of these models is a Newtonian fluid motion where the damper force is proportional to velocity. This can result in an inaccurate prediction of damper force at large amplitudes and high velocities, where under these conditions a non-Newtonian fluid behavior is experimentally observed to occur in the MR fluid.

This paper describes called the newly developed *Maxwell Nonlinear Slider* (MNS) model for modeling large-scale MR dampers. Characterization tests are conducted on a large-scale damper to identify the parameters for the MNS model. Comparisons are subsequently made between the behavior predicted by the MNS model and that measured while subjecting large-scale dampers to varying displacement and current histories. The results are shown to have better accuracy than existing models when applied toward the modeling of large-scale MR dampers.

2 MAXWELL NONLINEAR SLIDER MR DAMPER MODEL

The components of the MNS model are shown in Figure 1. The model has two modes: pre-yield and post-yield. In Figure 1, x is the degree of freedom of the model that is associated with the deformation of the damper, while y and z are variables associated with the pre-yield mode of the model. x and $\dot{x}$ are referred to as the *damper displacement* and the *damper velocity*, respectively, for simplicity. The variables x and y are related through the velocities $\dot{x}$ and $\dot{y}$ as well as the force f in the damper. The variables y and z are related through equilibrium with the damper force f applied to the model. One of the advantages of the MNS model is that the pre- and post-yield modes of response can be separated from each other, enabling the model parameters that describe these two modes of behavior to be independently identified. This makes it easier to identify the parameters for the model compared to other existing MR damper models.

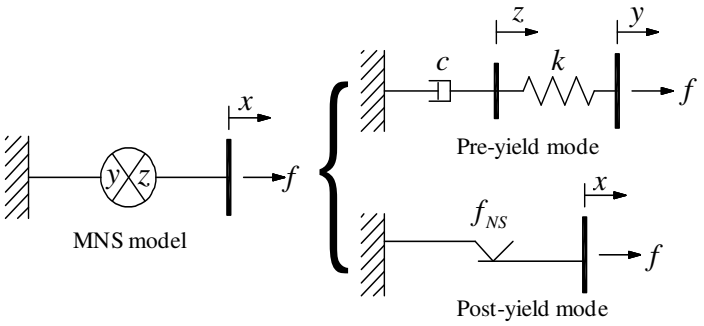

Figure 1. Proposed phenomenological MR damper model: Maxwell Nonlinear Slider (MNS) MR damper model

2.1 Pre-Yield Mode

During the pre-yield mode, the behavior of the damper is described by a Maxwell element, hence, the damper force f is determined by solving the following differential equation

$$f = k(y - z) = c\dot{z} \tag{1}$$

When the damper is in pre-yield mode, $\dot{y}$ is equal to the damper velocity $\dot{x}$. The initial value of y is set to be equal to x; thus Eq. 1 can be solved in terms of z for a given x and the damper force is then determined. The values of c and k for the Maxwell element are obtained from the force-velocity relationship observed in damper characterization tests, selecting two appropriate points on the hysteretic response curve and then applying visco-elasticity theory. Assuming the Maxwell element is subjected to a harmonic motion with an amplitude of u_0 and circular excitation frequency of ω, the coefficients c and k are calculated as follows:

$$c = \frac{1}{u_0\omega}\frac{f_0^2 + f_m^2}{f_m}, \qquad k = \frac{1}{u_0}\frac{f_0^2 + f_m^2}{f_0} \tag{2}$$

where f_0 and f_m are the damper force when the damper velocity is zero and a maximum value, respectively.

2.2 Post-Yield Mode

The post-yield behavior of the MNS model is described by the nonlinear slider which a frictional force defined by a set of post-yield curves that are pre-defined trajectories of the damper force on the force-velocity plane. In the post-yield mode the force is based on considering the damper velocity, i.e., $\dot{x}$. Figure 2 shows the post-yield curves for the MNS model, where a curve is defined for both a positive and negative force and referred to as the *positive* and *negative force post-yield curves*, respectively. Each post-yield curve is based on the Herschel-Bulkley model [13] and a linear line that is tangential to this curve at the velocity of $\dot{x}_t^+$ or $\dot{x}_t^-$, as shown in Figure 2. Since the Herschel-Bulkley model is incorporated into the MNS model, the property of a non-Newtonian fluid can be easily described by the MNS model. The mathematical representation of the positive force post-yield curve for the MNS model is given by

$$f_{py}^{+}(\dot{x}) = \begin{cases} a + b|\dot{x}|^{n} & \text{if } \dot{x} \geq \dot{x}_t^{+} \\ a_t(\dot{x} - \dot{x}_t^{+}) + f_t^{+} & \text{if } \dot{x} < \dot{x}_t^{+} \end{cases} \tag{3}$$

where a, b, n, and $\dot{x}_t^{+}$ are parameters to be identified from damper characterization tests; and $a_t = bn|\dot{x}_t^{+}|^{n-1}$ and $f_t^{+} = a + b|\dot{x}_t^{+}|^{n}$. The negative force post-yield curve, $f_{py}^{-}(\dot{x})$, can be defined in a similar manner as $f_{py}^{+}(\dot{x})$ using the appropriate values for the negative force post-yield curve parameters. The simplicity of the Herschel-Bulkley model enables values for the model parameters to be readily obtained from characterization tests since the post-yield behavior is independent of the identification of the Maxwell element parameters c and k that describe the pre-yield mode of the MNS model.

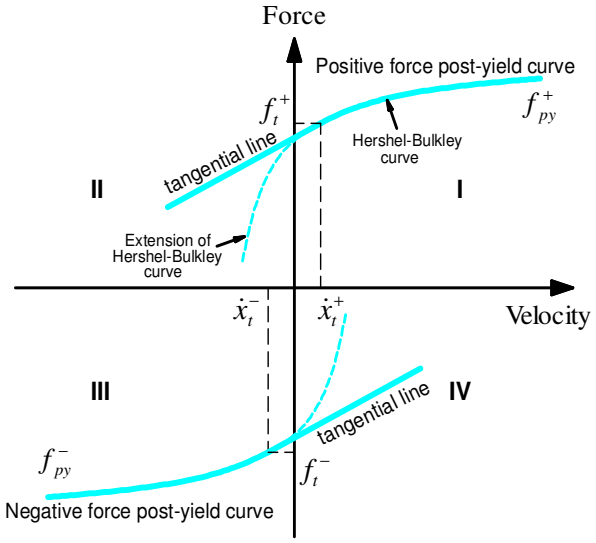

Figure 2. Pre-defined post-yield curves for MNS model

The post-yield curve is composed of two phases in the MNS model, namely, an *increasing phase* and *decreasing phase*. If the magnitude of the damper force is increasing during the post-yield mode, the damper is in the increasing phase. On the contrary, the damper is in the decreasing phase if the magnitude of the damper force is decreasing. Experimental data from the characterization tests show the trajectory of damper forces can be slightly different during the increasing and decreasing phase [14]. To account for this behavior, an inertial term is added to the post-yield damper force for the MNS model, whereby the force f in the damper is:

$$f = \begin{cases} f_{py}^{+}(\dot{x}) & \ddot{x} \geq 0; \text{increasing phase} \\ f_{py}^{+}(\dot{x}) + m_0\ddot{x} & \ddot{x} < 0; \text{decreasing phase} \end{cases} \tag{4}$$

where m_0 is a mass to account for the force discrepancy. When the damper force is on the negative force post-yield curve, the damper force is

$$f = \begin{cases} f_{py}^{-}(\dot{x}) & \ddot{x} < 0; \text{increasing phase} \\ f_{py}^{-}(\dot{x}) + m_0\ddot{x} & \ddot{x} \geq 0; \text{decreasing phase} \end{cases} \tag{5}$$

The value for the parameter m_0 can be obtained by equating the product of the measured acceleration and m_0 to the discrepancy between the post-yield mode measured damper force and the predicted force by the MNS model without the inertia term, where the measured quantities are from damper characterization tests.

2.3 Criteria for Mode Change

When the damper force f from the Maxwell element reaches the post-yield curve, the nonlinear slider is activated and the mode changes from the pre-yield to the post-yield state. Mathematically, this condition is expressed as

$$|f| = |f_{py}(\dot{x})| \tag{6}$$

Equation 6 implies that the generated damper force is always bounded by the positive and negative force post-yield curves in the MNS model. The transition from the post-yield mode to the pre-yield mode occurs when the following velocity equation is satisfied during the post-yield mode

$$\dot{x} = \dot{y} \tag{7}$$

where, $\dot{y}$ is calculated from

$$\dot{y} = \frac{\dot{f}}{k} + \frac{f}{c} \tag{8}$$

Equation (8) is obtained by solving for y from Eq. (1) and then taking the time derivative of y. The value for $\dot{y}$ is then calculated by substituting the damper force f and the time derivative of the damper force, $\dot{f}$, from the post-yield mode into Eq. (8). To obtain a smooth transition from the post-yield mode to the pre-yield mode, during the post-yield mode the pre-yield mode variables y and z of the model are continuously updated by solving Eq. (1) for z and y using the force f developed in the damper during the post-yield mode.

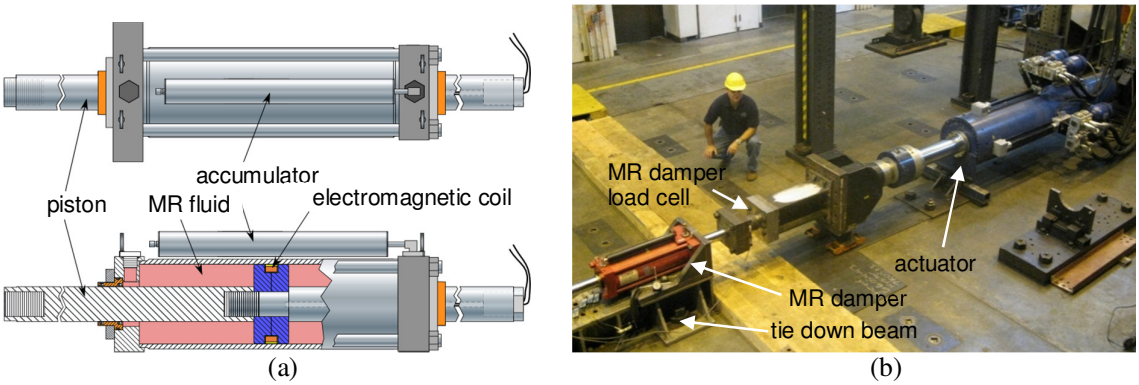

(a) (b)

Figure 3. (a) Schematic of a large-scale MR damper by Lord Corporation (after Bass and Christenson 2007); (b) experimental setup for the characterization test of MR damper

3 DAMPER CHARACTERIZATION TESTS

Characterization tests were performed at the Lehigh NEES equipment site on a large-scale MR damper. The damper is manufactured by Lord Corporation and is similar to the MR dampers used by Bass and Christenson [8] in their research. The damper is shown schematically in Figure 3(a). The length and available stroke of the damper are 1.5m and ±279mm, respectively. The electromagnetic coil consists of 368 turns of 18 AWG magnet wire with an annular gap of 1.0 mm between the piston head and the inside diameter of the cylinder. The damper is filled with approximately 19 liters of MRF-132DG type MR fluid manufactured by Lord Corporation.

The experimental setup for the characterization test consists of primary two parts: i) a hydraulic actuator to control the movement of the MR damper; and ii) electrical hardware to supply an appropriate current to the damper for the control of the damper force. Figure 3(b) shows the test setup for the characterization test of the MR damper. The MR damper is connected to the hydraulic actuator through a stiff horizontal steel section. This is done in order to extend the arm of the actuator piston to accommodate the spacing of anchor locations for threaded rods that secure the damper and actuator to the laboratory strong floor. The maximum force capacity of the actuator is 1,700kN; with the actuator having the ability to generate approximately 500kN of force at a piston velocity of 1.0m/sec. A 534kN load cell is installed between the horizontal steel section and the damper piston to directly measure the force developed in the damper.

The current going into the damper is controlled by a pulse width modulation (PWM) type current driver manufactured by Advanced Motion Controls (30A8). The PWM servo-amplifier can supply the current to the electrical circuit up to 30A by driving the DC motor at a high rate of switching frequency (22kHz). To reduce the noise from the electrical power source, a Schaffner line filter is deployed in front of the DC power supply that provides 72 DC voltage to the PWM servo-amplifier. The command current is transferred to the PWM servo-amplifier through voltage signals from -10V to +10V to produce the desired current utilizing pulse width modulation. The current going into the MR damper is monitored by a current probe (CR Magnetics current transformer).

Table 1. Identified parameters for MNS damper model

Current, I (Amps)	c (kN s/m)	k (kN/m)	Positve force post-yield curve				Negative force post-yield curve				m_0 (kN s^2/m)
			a (kN)	b (kN s/m)	n	$\dot{x}_t^+$ (m/s)	a (kN)	b (kN s/m)	n	$\dot{x}_t^-$ (m/s)	
0.0	10,000	100,000	7.5	243.5	1.62	0.010	-7.3	-235.6	1.60	-0.010	0.50
0.5	11,000	100,000	53.1	162.5	0.85	0.010	-53.1	-162.5	0.85	-0.010	0.50
1.0	12,000	118,000	91.5	122.5	0.52	0.010	-96.0	-134.9	0.60	-0.010	1.60
1.5	12,000	118,000	126.7	152.1	0.58	0.010	-126.7	-152.1	0.58	-0.010	1.50
2.0	11,491	110,030	148.5	166.3	0.66	0.003	-146.8	-182.1	0.71	-0.003	1.05
2.5	12,278	112,890	138.5	161.8	0.46	0.017	-133.5	-171.8	0.46	-0.012	1.04

The parameters for the MNS damper model are identified in such a manner that a minimal error is achieved between the damper force predicted by the model and that measured during the characterization tests. In this paper the particle swarm optimization (PSO) algorithm by Kennedy and Eberhart [15] is used for the identification of the damper model parameters. The normalized root mean square (RMS) error by Gavin [11] is used as the objective function that is minimized to establish the values of the model parameters. The parameters are obtained for a range of selected currents from various characterization tests involving sinusoidal displace-

ment histories. For each current level, four different sinusoidal tests with the amplitude of 25.4mm and frequencies of 0.5Hz, 1.0Hz, 2.0Hz, and 3.0Hz were conducted for the identification of the model parameters. Table 1 shows the identified parameters of the MNS model for the various current levels. To compare the performance of the MNS model with the Bouc-Wen and hyperbolic tangent models the parameters for these other models are also identified using the PSO applied to the same experimental data set.

4 EXPERIMENTAL EVALUATION OF MNS MODEL UNDER CONSTANT CURRENT

The MNS model was evaluated by comparing the damper response predicted by the model with that recorded in tests where the displacement history was based on selected Gaussian white noise (see Figure 4(a) and Table 2). The comparisons are shown in Figure 4(b), (c) and (d), where the damper force time history, damper force-displacement, and damper force-velocity are given, respectively. The current input, I, for the damper is constant and equal to 2.5A for the results shown in Figure 4. Good agreement between the MNS model and the test results is evident in Figure 4.

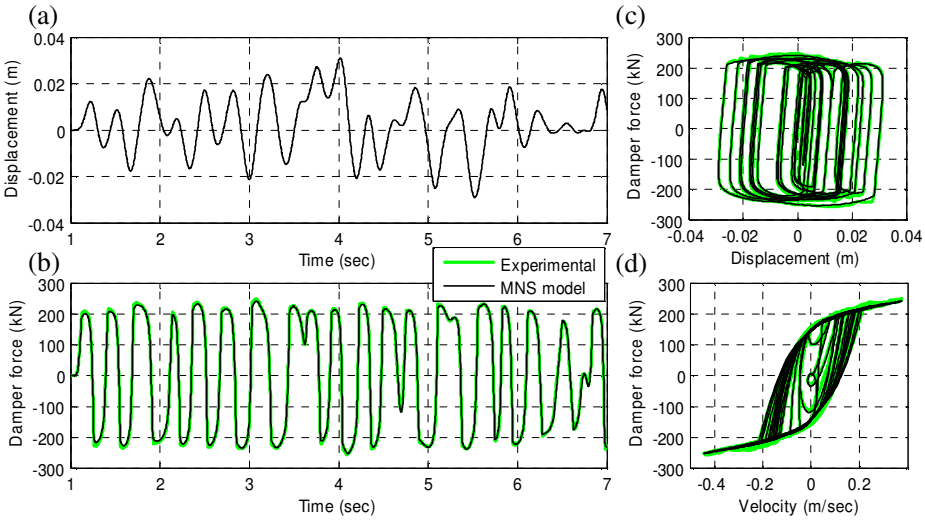

Figure 4. Comparison of predicted damper force by MNS model with experimental data (I=2.5A): (a) time history of input displacement; (b) time history of damper force; (c) force-displacement relationship; (d) force-velocity relationship.

Table 2. Comparison of normalized RMS error of MR damper models with band-limited Gaussian white noise

Damper Current I (Amps)	Gaussian white noise (displacement input)			Normalized RMS error		
	Max. disp. (m)	Max. velocity (m/s)	Bandwidth (Hz)	Bouc-Wen model	Hyperbolic tangent model	MNS model
0.0	0.050	0.452	2.0	0.1291	0.0992	0.0688
2.5	0.030	0.445	4.0	0.0420	0.0409	0.0370

Table 2 presents a comparison of the normalized RMS error [11] for the MNS, Bouc-Wen, and hyperbolic-tangent damper models for two cases involving a constant current input of I=0.0A and 2.5A. For the cases with I=0.0A and 2.5A the displacement history is based on Gaussian white noise with a bandwidth of 2Hz and 4Hz, respectively. As can be seen in Table 2, the MNS model shows better agreement with the test data than with the Bouc-Wen and hyperbolic-tangent models.

5 DYNAMICS OF MR DAMPER ASSOCIATED WITH VARIABLE CURRENT

5.1 Dynamics of Current Driver (PWM Servo-Amplifier)

Due to the inductance of the electro-magnetic coil that generates the magnetic field in the damper, the current within the electro-magnetic circuit changes slowly if a voltage driven power supply is used [12]. To overcome this problem, a PWM servo-amplifier with a PI controller is often used. Yang presented a governing differential equation for the electro-magnetic circuit based on the duty cycle of a PWM servo-amplifier and PI controller [6]. In this paper the same governing equation is used, from which a transfer function *G(s)* between the current output to the damper and current command signal for the current driver is derived:

$$G(s) = \frac{235s + 44522}{s^2 + 302s + 44522} \tag{9}$$

5.2 Dynamics of Electromagnetism

As noted previously, numerous semi-active control algorithms have been developed for MR dampers. These control laws involve supplying a variable current command to the damper. To understand the dynamics of an MR damper, it is necessary to investigate the dynamic behavior of the magnetic field in the damper associated with variable current. When the current changes inside the electromagnetic coil, a magnetic flux that is proportional to the current in the coil is generated. The magnetic flux induces eddy currents in the material around the coil (e.g., the piston head, cylinder housing), which opposes the magnetic flux generated by the coil according to Lenz's law. This results in the development of a time delay in the MR damper force under a variable current input [16]. The hysteresis of the magnetization of the MR damper fluid makes it difficult to predict the damper force, for the piston head and cylinder housing around the coil can develop a residual magnetic field after the applied magnetic field has been removed. This nonlinear hysteretic behavior not only can affect the induction of eddy currents, but it can also disturb the formation of the total magnetic field and the damper force. Therefore, the use of a first order filter [9] for the description of the dynamics of a MR damper may not be sufficient to explain the complex behavior of an MR damper under a variable current input. To obtain a better prediction of the damper force under variable current, this paper proposes a model based on the following nonlinear differential equation to relate the coil current to an equivalent static current:

$$\dot{I}_{eq} = \alpha(\dot{I}_r)(I - I_{eq}) \tag{10}$$

The function $\alpha()$ is determined from the Eqs. (11) and (12):

$$\alpha(\dot{I}_r) = \begin{cases} a^+\dot{I}_r + \alpha_1 & \text{if } \dot{I}_r \geq 0 \\ a^-\dot{I}_r + \alpha_1 & \text{if } \dot{I}_r < 0 \end{cases} \tag{11}$$

$$\dot{I}_r = \alpha_0(I - I_r) \tag{12}$$

where, α_0, α_1, a^+ and a^- are constants which are obtained by utilizing nonlinear optimization theory to minimize the error between the predicted and experimental response of the damper force. I is the current in the coil, which is generated by the current driver. I_{eq} is an equivalent static current that can generate the same magnetic flux as the resultant magnetic flux at time t created by I, the eddy currents, residual magnetic fields, and other phenomena that affect the formation of the magnetic flux.

The MNS model with the Eqs. (9) and (10) to account for the effect of variable current input is referred to as the *variable current MNS model*. Figure 5 shows the block diagram for the variable current MNS model. With I_{eq} obtained from the solution to Eq. (10), the parameter sets in Table 1 can be interpolated or directly used under variable current inputs to specify the damper parameters for the model which enables the damper force to be calculated using the MNS model.

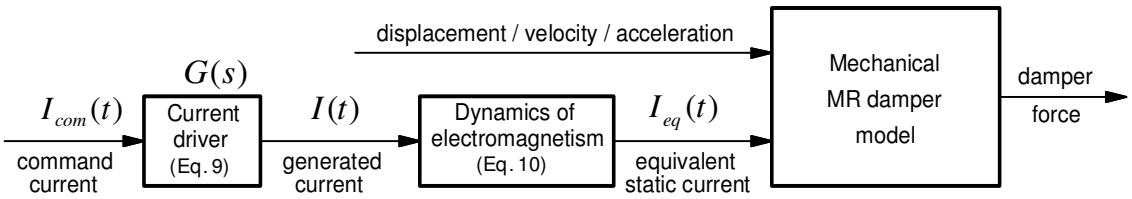

Figure 5. Block diagram for MR damper model under variable current

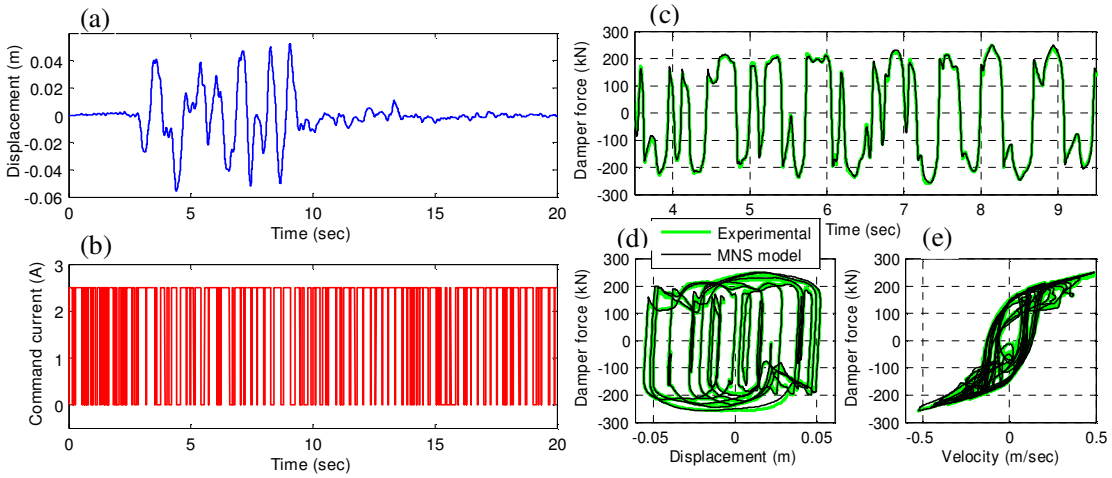

Figure 6. Response of large-scale MR damper under variable current: (a) time history of input displacement; (b) time history of input current; (c) time history of damper force; (d) force-displacement relationship; (e) force-velocity relationship.

To assess the model, tests with variable displacement and current were performed, where the variation in current simulated that from the clipped optimal controller algorithm with a maximum current of 2.5A. Figure 6 (a) and (b) show the pre-defined displacement and current time histories for the MR damper. The experimental response and MNS model prediction of the MR damper are shown in Fig. 6 (c) through (e). The values for the parameters for Eqs. 10, 11, and 12 are: $\alpha_0 = 24.96$, $\alpha_1 = 3.57$, $a^+ = 0.31$, $a^- = -0.30$. As can be observed in Figure 6, the MNS model can accurately predict the response of the MR damper under variable current.

In order to further validate the variable current MNS model, a real-time hybrid simulation of a 3-story building with the large-scale MR damper was conducted [17]. The experimental response of the damper was compared with the results from a numerical simulation involving the variable current MNS model. The building was subjected to the 1989 Loma Prieta earthquake ground motion scaled to the design basis earthquake (DBE) having about a 475 year return period [18]. The sliding mode control (SMC) [19] was used for the semi-active control of the MR damper. As can be observed in Figure 7, the damper force predicted by the variable current MNS model in the numerical simulation (denoted as *Numerical* in Figure 7) matches well with the measured experimental damper force obtained from the real-time hybrid simulation (denoted as *RTHS* in Figure 7); the command current from the numerical simulation also shows good agreement with that from the real-time hybrid simulation. The results shown in Figure 6 and 7 demonstrate the robustness and accuracy of the variable current MNS MR damper model.

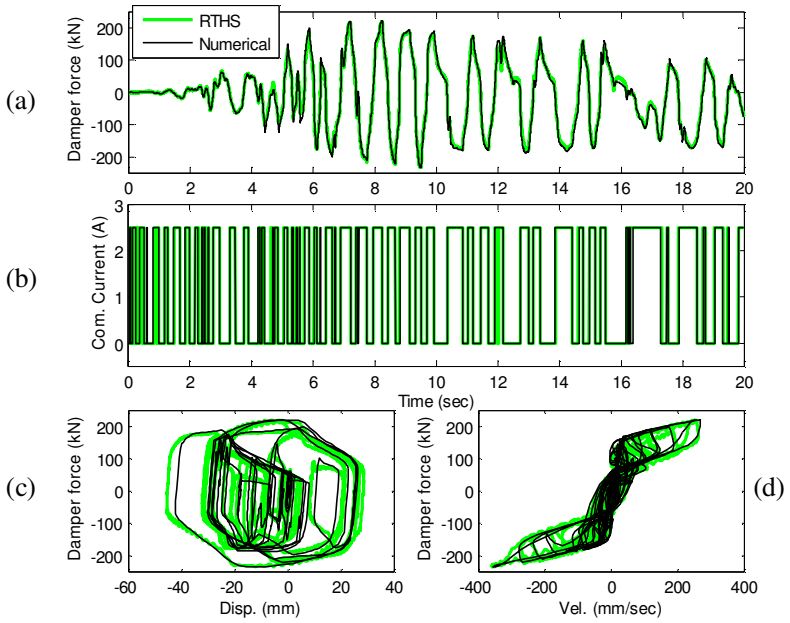

Figure 7 Comparison of damper response under the 1989 Loma Prieta earthquake ground motion with sliding mode controller: (a) time history of damper force; (b) time history of command current; (c) force-displacement relationship; (d) force-velocity relationship

6 CONCLUSIONS

A newly developed formulation called the variable current Maxwell Nonlinear Slider model was presented for the prediction of the dynamic behavior of large-scale MR dampers under variable current. In the Maxwell Nonlinear Slider model, the pre-yield and post-yield behaviors of an MR damper are independently described. This simplifies the identification of the model parameters from characterization tests. The Maxwell Nonlinear Slider model utilizes the Hershel-Bulkley model to describe the post-yield behavior, thereby enabling the property of a non-Newtonian fluid to be readily included in the Maxwell Nonlinear Slider model and the effects of shear thinning and thickening behavior of the MR fluid to be accounted for. The solution to a nonlinear differential equation is used to account for the time lag response of the MR damper force that occurs under with a variable current input. Predictions made by the Maxwell Nonlinear Slider model under constant and variable current inputs show good

agreement with experimental results. Further studies of the dynamics of MR dampers needs to be conducted in order to evaluate and calibrate the formulation over a wider range of variable current inputs, as well as frequencies and amplitudes in the displacement history than those presented in this paper.

ACKNOWLEDGEMENTS

This paper is based upon work supported by grants from the Pennsylvania Department of Community and Economic Development through the Pennsylvania Infrastructure Technology Alliance, and by the National Science Foundation under Grant No. CMS-1011534 within the George E. Brown, Jr. Network for Earthquake Engineering Simulation Research (NEESR) program, Award No. CMS-0612661, and Award No. CMS-0402490 NEES Consortium Operation.. The MR fluid dampers were provided by Dr. Richard Christenson at the University of Connecticut. The authors appreciate his support.

REFERENCES

[1] Dyke, S.J., Spencer Jr., B.F., Sain, M.K. and Carlson, J.D., Modeling and control of magneto-rheological dampers for seismic response reduction, *Smart Materials and Structures*, **5**, 565-575, 1996.

[2] Jansen, L.M. and Dyke, S.J., Semi-active control strategies for MR dampers: comparison study, *Journal of Engineering Mechanics*, **126**(8), 795-803, 2000.

[3] Schurter, K. C. and Roschke, P. N., Neuro-fuzzy control of structures using acceleration feedback, *Smart Materials and Structures*, **10**, 770-779, 2001.

[4] Ribakov, Y. and Gluck, J., Selective controlled base isolation system with magneto-rheological dampers, *Earthquake Engineering and Structural Dynamics*, **31**, 1301-1324, 2002.

[5] Carlson, J. D., and Spencer, B. F., Jr., Magneto-rheological fluid dampers for semi-active seismic control, *Proc., 3rd Int. Conf. on Motion and Vibration Control*, **3**, Chiba, Japan, 35–40, 1996.

[6] Yang, G., Large-Scale Magneto-rheological fluid damper for vibration mitigation: modeling, testing and control, *Ph.D. Dissertation*, Department of Civil Engineering and Geological Sciences, University of Notre Dame, Notre Dame, Indiana, 2001.

[7] Sodeyama, H., Suzuki, K. and Sunakoda, K., Development of large capacity semi-active seismic damper using magneto-rheological fluid, *Journal of Pressure Vessel Technology*, **126**, 105-109, 2004.

[8] Bass, B. J., and Christenson, R. E., System identification of a 200 kN, magneto-rheological fluid damper for structural control in large-scale smart structures, *Proc., Amer. Control Conf.*, NY, 2007.

[9] Spencer, B. F., Dyke, S. J., Sain, M. K. and Carlson, J. D., Phenomenological model for magneto-rheological dampers, *Journal of Engineering Mechanics*, **123**(3), 230-238, 1997.

[10] Butz, T and Von Stryk, O., Modelling and simulation of electro- and magneto-rheological fluid dampers, *ZAMM - Journal of Applied Mathematics and Mechanics*, **82**, 3-20, 2002.

[11] Gavin, H.P., Multi-duct ER dampers, *Journal of Intelligent Material Sys and Structures*, **12**, 353-366, 2001.

[12] Yang, G., Spencer Jr., B. F., Carlson, J. D., Sain, M. K., Large-scale MR fluid dampers: modeling and dynamic performance considerations, *Engineering Structures*, **24**, 309-323, 2002.

[13] Herschel, W.H. and Bulkley, R., Konsistenzmessungen von Gummi-Benzollösungen, Kolloid Zeitschrift, **39**, 291–300, 1926.

[14] Chae, Y., Seismic hazard mitigation of building structures using magneto-rheological dampers, *Ph.D. Dissertation*, Lehigh University, Bethlehem, PA, 2011.

[15] Kennedy, J. and Eberhart, R. C., Particle swarm optimization, *IEEE Int. Conf. on Neural. Networks (Perth)* , **4**, 1942–1949, 1995.

[16] Takesue, N., Furusho, J. and Kiyota, Y., Fast response MR-fluid actuator, *JSME International Journal Series C*, **47**(3), 783-791, 2004.

[17] Chae, Y., Ricles, J.M., Sause, R., Dong, B., Chen, C., Christenson, R., Dyke, S.J., Agrawal, A., and Spencer, B.F., Experimental studies on control strategies for steel frames with MR dampers for earthquake hazard reduction, *5th World Conference on Structural Control and Monitoring*, Japan, 2010.

[18] Federal Emergency Management Agency *NEHRP Recommended Provisions for Seismic Regulations for New Buildings and Other Structures, Part 1- Provisions and Part 2 – Commentary,* Report No. FEMA-450, Washington, D.C., 2003.

[19] Utkin, V.I. *Sliding Modes in Control Optimization* Springer-Verlag, New York, 1992.